nature photonics

LETTERS

https://doi.org/10.1038/s41566-017-0026-y

Self-starting harmonic frequency comb generation in a quantum cascade laser

Dmitry Kazakov[1,2], Marco Piccardo[1*], Yongrui Wang[3], Paul Chevalier[1], Tobias S. Mansuripur[4], Feng Xie[5], Chung-en Zah[5], Kevin Lascola[5], Alexey Belyanin[3] and Federico Capasso[1*]

Optical frequency combs[1,2] establish a rigid phase-coherent link between microwave and optical domains and are emerging as high-precision tools in an increasing number of applications[3]. Frequency combs with large intermodal spacing are employed in the field of microwave photonics for radio-frequency arbitrary waveform synthesis[4,5] and for the generation of terahertz tones of high spectral purity in future wireless communication networks[6,7]. Here, we demonstrate self-starting harmonic frequency comb generation with a terahertz repetition rate in a quantum cascade laser. The large intermodal spacing caused by the suppression of tens of adjacent cavity modes originates from a parametric contribution to the gain due to temporal modulations of population inversion in the laser[8,9]. Using multiheterodyne self-detection, the mode spacing of the harmonic comb is shown to be uniform to within 5×10^{-12} parts of the central frequency. This new harmonic comb state extends the range of applications of quantum cascade laser frequency combs[10–13].

In recent decades, several techniques to generate optical frequency combs (OFCs) have been demonstrated based on different nonlinear mechanisms that fulfil the mode-locking condition. Originally, passively mode-locked lasers based on saturable absorption and Kerr lensing were used to create short light pulses, and were subsequently shown to also constitute frequency combs. This type of mode locking is an example of amplitude-modulated mode locking, so-named for the temporal behaviour of the electric field of the emitted light. However, these techniques usually result in elaborate optical systems. More recently, new routes promising chip-scale comb generators have been investigated based on optically pumped ultrahigh-quality-factor crystalline microresonators[14–16] and broadband quantum cascade lasers (QCLs) with specially designed multistage active regions[10,17]. In both cases, the essential underlying mechanism responsible for the generation of OFCs is cascaded four-wave mixing (FWM) enabled by a third-order $\chi^{(3)}$ Kerr nonlinearity. The temporal behaviour of these OFCs is not restricted to ultrashort pulses, but can represent rather sophisticated waveforms due to a non-trivial relationship among the spectral phases of the comb teeth. In fact, the output of a QCL-based frequency comb resembles that of a frequency-modulated laser with nearly constant output intensity[10,18].

A novel mechanism of OFC generation in QCLs was suggested by the recent discovery of a new laser state[19], which comprises many modes separated by higher harmonics of the cavity free spectral range (FSR) (Fig. 1a). Its spectrum differs radically from that of QCLs in fundamental comb operation, where adjacent cavity modes are populated (Fig. 1b). This new state is achieved by controlling the current so that the QCL first reaches a state of high single-mode intracavity intensity. When this intensity is large enough, an instability threshold is reached caused by the $\chi^{(3)}$ population pulsation nonlinearity, favouring the appearance of modes separated by tens of FSRs from the first lasing mode. In this Letter, we verify the equidistance of these modes, thereby proving that QCLs are capable of harmonic comb operation and concomitant high-repetition-rate OFC generation. OFCs with repetition frequencies ranging between 10 and 1,000 GHz have already been demonstrated in optically pumped microresonators[14], but the generation of high-repetition-rate OFCs based on QCLs operating in the harmonic regime presents the advantage of a truly monolithic, electrically driven source. It is notable that this type of comb operation does not require additional intracavity nonlinear elements such as saturable absorbers, or mode-selection elements such as Bragg reflectors, which were used to achieve passive harmonic mode locking at terahertz repetition rates in other semiconductor lasers[20]. Instead, the modes are locked passively due to the behaviour of the QCL gain medium itself.

Here, we use two Fabry–Pérot (FP) QCLs fabricated from the same growth process with 6-mm-long cavities and emitting at 4.5 μm (see Methods for details). These devices exhibit four distinct laser states as a function of the injected current (Fig. 2a). Starting from single-mode operation and slowly increasing the bias, one can observe the harmonic state appearing at a pump current only fractionally higher than the lasing threshold. No beatnote at the cavity roundtrip frequency (f_{rt}) is observed in this regime (Fig. 2b), confirming the absence of interleaving FP modes.

At higher values of injected current, the laser transitions to a single-FSR-spaced state producing a single narrow intermodal beatnote (full-width at half-maximum, FWHM < 1 kHz) at f_{rt}, indicating the occurrence of fundamental comb operation[10]. At even higher current, the single-FSR comb acquires a high-phase-noise pedestal—a typical signature of comb destabilization[21]. To verify the spacing uniformity of the modes of the harmonic state, techniques developed to investigate combs with an intermodal spacing in the lower gigahertz range (such as intermode beat spectroscopy[10] and shifted wave interference Fourier transform spectroscopy[12]) cannot be applied because the terahertz-scale beatnote frequency of the harmonic state is beyond the

[1]Harvard John A. Paulson School of Engineering and Applied Sciences, Harvard University, Cambridge, MA 02138, USA. [2]Department of Information Technology and Electrical Engineering, ETH Zurich, 8092 Zurich, Switzerland. [3]Department of Physics and Astronomy, Texas A&M University, College Station, TX 77843, USA. [4]Pendar Technologies, 30 Spinelli Place, Cambridge, MA 02138, USA. [5]Thorlabs Quantum Electronics (TQE), Jessup, MD 20794, USA. Dmitry Kazakov and Marco Piccardo contributed equally to this work. *e-mail: piccardo@g.harvard.edu; capasso@seas.harvard.edu

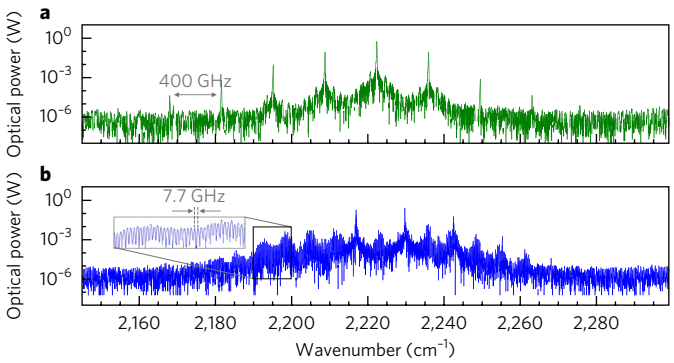

Fig. 1 | Harmonic and fundamental comb operation in QCLs. a, Optical spectrum of a mid-IR QCL in the harmonic state with a repetition rate of 400 GHz. **b**, Optical spectrum of a QCL in fundamental comb operation with a repetition rate of 7.7 GHz. In both cases, the cavity free spectral range is 7.7 GHz.

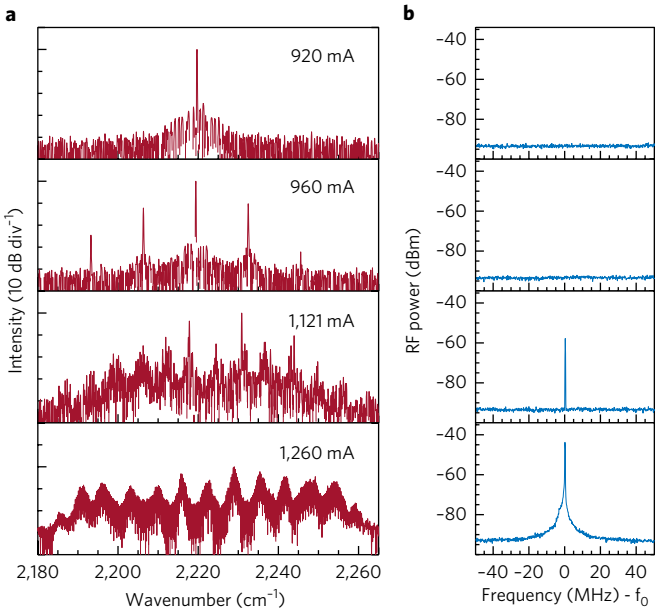

Fig. 2 | Spectral evolution of FP QCLs. a, Optical spectra corresponding to different laser states (from low to high current): single mode, harmonic frequency comb, fundamental frequency comb and high-phase-noise state. **b**, Corresponding RF spectra acquired at the QCL cavity roundtrip frequency (f_0 = 7.6776 GHz at 920, 960 and 1,121 mA, and 7.6678 GHz at 1,260 mA, resolution bandwidth = 200 kHz). The absence of the intermodal beatnote in the harmonic state (960 mA) signifies the suppression of adjacent FP modes. The narrow beatnote at the cavity FSR is a signature of comb operation and appears when neighbouring FP modes start lasing (1,121 mA). At 1,260 mA, the comb is destabilized and the beatnote features a high-phase-noise pedestal.

bandwidth of conventional mid-infrared (mid-IR) detectors and radiofrequency (RF) electronics. Instead, we use a technique that was first developed to characterize high-repetition-rate microresonator combs, in which the sample comb spectrum is downconverted from the optical to the RF domain by means of multiheterodyne beating with the modes of a finely spaced reference comb[22]. In this scheme, if the harmonic state constitutes a frequency comb, the downconverted spectrum will form an RF comb whose equidistant spacing can be accurately verified using electronic frequency counters.

For the multiheterodyne experiment we used two QCLs, one operating in the harmonic comb regime (QCL_1) and the other in a fundamental comb regime (QCL_2) acting as a reference comb with an intermodal spacing of ~7.7 GHz. We employed a self-detection scheme in which the light emitted from QCL_1 is injected, after passing through an optical isolator, into the cavity of QCL_2 (Fig. 3f). The latter acts at the same time as a reference comb and a fast photomixer[23], from which we can extract electrically the multiheterodyne signal generated by the intracavity beating of the optical fields of the two lasers. The attractive feature of this scheme is that it provides better signal stability than a standard approach utilizing an external fast photodiode. A description of this method is provided in the Supplementary Information, and its results are shown for comparison in Fig. 3g,h.

The emission spectra of the harmonic and reference comb measured using the self-detection scheme are presented in Fig. 3a,b. QCL_1 is operating in the harmonic comb regime, while QCL_2 is operating in a fundamental comb regime exhibiting adjacent cavity modes that constitute an equidistant grid with a spacing defined by f_{rt} (Fig. 3c,d). Interestingly, several prominent peaks not lying on this grid can be identified in the spectrum of QCL_2 (marked by green arrowheads in Fig. 3b–d), corresponding to modes injected from QCL_1 into QCL_2. The pairwise beating of the modes of the harmonic state with the nearest modes of the reference comb produces the multiheterodyne spectrum shown in Fig. 3e.

To assess the locking of the harmonic modes we further downconverted the multiheterodyne signal with an RF mixer and selected three beatnotes of the spectrum using bandpass filters whose outputs were fed into three synchronized frequency counters. From the measured frequencies, a histogram showing the statistics of the deviation from equidistant spacing of the RF comb can be constructed (Fig. 3g). The fractional frequency stability of the dual-comb system exhibits an inverse square-root dependence on the averaging time, indicating the dominance of white-noise frequency modulations in the system giving rise to random and uncorrelated fluctuations following a normal distribution (Fig. 3h). This allows the histogram to be fit with a Gaussian function, which yields a mean value of $\mu = -27$ Hz and a standard deviation of $\sigma = 329$ Hz. This result verifies the equidistant spacing of the harmonic comb with a relative accuracy of $\sigma/f_c = 5 \times 10^{-12}$, as normalized to the optical carrier frequency of the laser (f_c = 66.7 THz), being an order of magnitude smaller than for the measurement based on external detection. This net improvement is due to the higher stability of the multiheterodyne signal in the self-detection scheme (Fig. 3h), as discussed in Supplementary Section IIC.

To explain the occurrence of harmonic comb operation we resort to a perturbation theory of comb formation in QCLs considering the interaction of a two-level gain medium with a field comprising a central mode and two weak equally detuned sidebands in the laser cavity. The nature of the parametric gain responsible for adjacent mode skipping in the laser was studied in ref. [19]. Here, we apply a more general approach that includes, in a systematic way, the effects of nonequal sideband amplitudes, diffusion of the population grating and group velocity dispersion (GVD), which may hamper comb operation[21]. The complete derivation of our theory is provided in Supplementary Section III, while here we outline the main implications given by the solutions of our model for the real device parameters. The subthreshold GVD of QCL_1, measured by a standard technique[24], is displayed in Fig. 4a. The net parametric gain calculated as a function of sideband detuning is shown in Fig. 4b. It peaks at a frequency of 200 GHz (26 FSR of a 6-mm-long cavity)

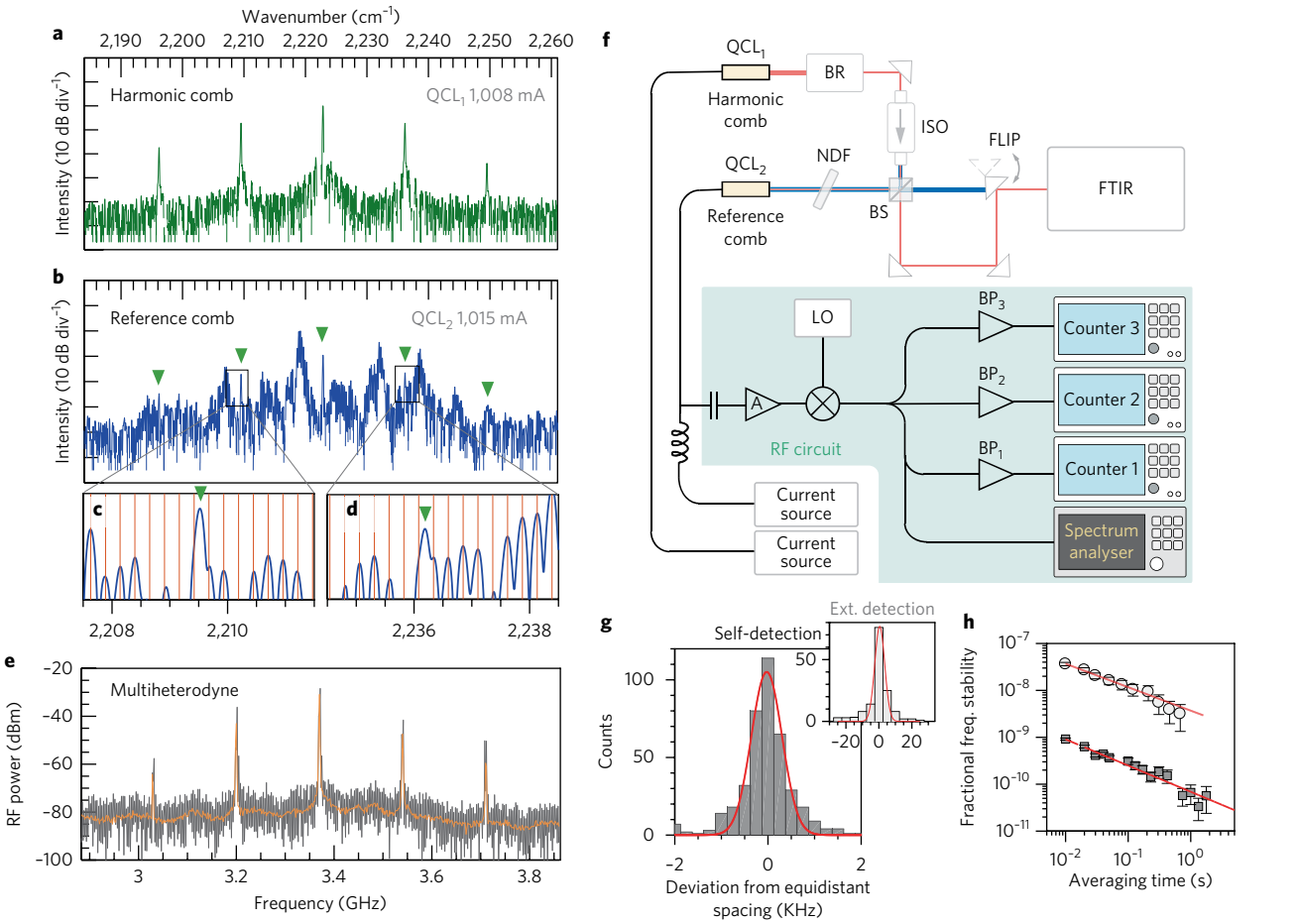

Fig. 3 | Mode spacing uniformity of the harmonic state. a, Optical spectrum of QCL_1 in the harmonic regime. **b**, Optical spectrum of QCL_2 (reference comb) upon optical injection from QCL_1. **c**,**d**, Magnified views of a portion of the spectrum of QCL_2. **e**, Multiheterodyne spectrum produced by pairwise beating of the nearest modes of the two lasers. The orange trace represents the spectrum averaged over 1,000 sweeps of 2 ms. **f**, Optical and RF set-up for assessment of the comb nature of the harmonic state. BR, beam reducer; ISO, optical isolator; BS, beamsplitter; FLIP, flip mirror; NDF, neutral density filter; BP, bandpass filter; LO, local oscillator; A, amplifier; FTIR, Fourier transform infrared spectrometer. The RF mixer is used to downconvert the multiheterodyne signal and align the beatnotes within the passbands of the electrical filters by changing the local oscillator frequency. **g**, Histogram showing the deviation from equidistant spacing of the harmonic state measured with the set-up shown in **f** for a gate time of 10 ms and 402 counts. The parameters of the Gaussian fit (red curve) are $\mu = -27$ Hz and $\sigma = 329$ Hz. Inset: Histogram obtained with the same technique while beating on an external detector. **h**, Fractional frequency stability of the dual-comb system in self-detection mode (squares) versus external detection mode (circles). The self-detected system shows more than an order of magnitude improvement in frequency stability. Error bars are defined as the confidence interval corresponding to one standard deviation.

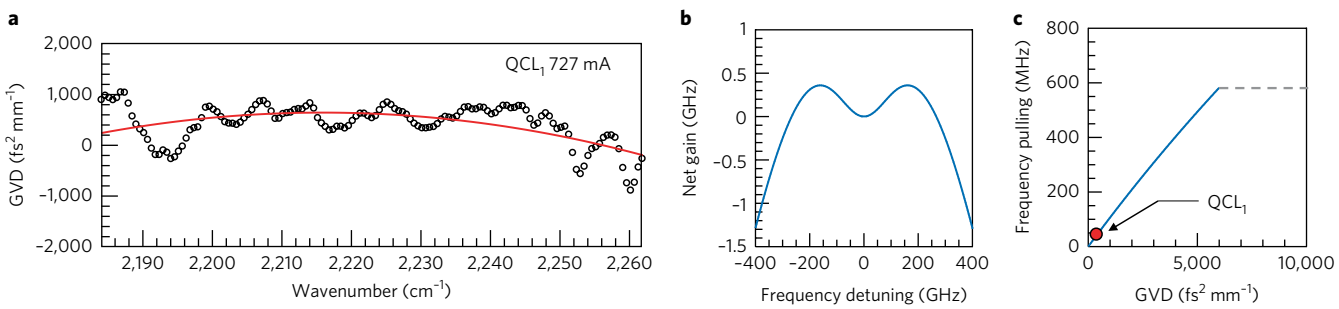

Fig. 4 | Harmonic comb operation in presence of native dispersion. a, Measured subthreshold GVD of QCL_1. Experimental data (open circles) are fitted with a parabola (red curve). **b**, Net gain predicted by the perturbation theory of harmonic comb formation using the device parameters of QCL_1, including the measured subthreshold GVD. **c**, Calculated frequency pulling exerted by FWM processes occurring in the QCL and compensating the dispersion of the laser as a function of subthreshold GVD (continuous blue line), a phenomenon theoretically treated in Supplementary Section III. Above 6,000 fs^2 mm^{-1}, FWM cannot compensate for the laser dispersion (dashed grey line), preventing the occurrence of harmonic comb operation. The GVD value of QCL_1 is shown for reference (red circle).

with respect to the central mode, indicating that the modes at this frequency are the first to oscillate, while the modes lying closer to the central pump are parametrically suppressed. Furthermore, we calculate that FWM can compensate for the non-zero dispersion of the real device up to a GVD of 6,000 $fs^2\,mm^{-1}$, above which the onset of harmonic comb operation is hampered (Fig. 4c). These results are consistent with our experimental findings proving the occurrence of harmonic comb operation in a QCL with a GVD below 1,000 $fs^2\,mm^{-1}$.

The ability to generate and passively lock harmonic modes while skipping adjacent cavity resonances relies on a coherent instability enabled by the QCL gain medium, unveiling the compelling dynamics of the new laser state in QCLs. Locking of comb teeth with a spacing comparable to the gain recovery frequency represents a major step towards the demonstration of coherent mid-IR amplitude-modulated waveform emission from QCLs, long thought to be prevented by the underlying physical principles, and paving the way towards applications requiring short pulses of mid-IR light.

In this respect, an important point to address in future studies is measurement of the relative phases of the harmonic modes, which may be achieved by means of a multiheterodyne experiment involving a reference comb with known spectral phase or using spectrum analyser extension modules in the terahertz range. On the other hand, QCL harmonic comb generators may find applications in future wireless terahertz communication networks[25], as they combine the functionality of a high-bandwidth photomixer and a comb source, promising the intracavity generation of powerful terahertz carrier signals, whose frequency can be designed by engineering the facet coatings of the device[19] and where the phase noise is inherently low due to a high degree of correlation among the optical modes that produce the beatnote. Merging this capability with the fact that QCLs can be optimized to have a flat frequency response over a large modulation bandwidth[26] may allow them to operate as compact unibody modems to transmit and receive digital data in the terahertz communication band.

Methods

Methods, including statements of data availability and any associated accession codes and references, are available at https://doi.org/10.1038/s41566-017-0026-y.

Received: 9 June 2017; Accepted: 14 September 2017;
Published online: 16 October 2017

References

1. Udem, T., Holzwarth, R. & Hänsch, T. W. Optical frequency metrology. *Nature* **416**, 233–237 (2002).
2. Hänsch, T. W. Nobel lecture: Passion for precision. *Rev. Mod. Phys.* **78**, 1297–1309 (2006).
3. Diddams, S. A. The evolving optical frequency comb. *J. Opt. Soc. Am. B* **27**, B51 (2010).
4. Huang, C.-B., Jiang, Z., Leaird, D. E., Caraquitena, J. & Weiner, A. M. Spectral line-by-line shaping for optical and microwave arbitrary waveform generations. *Laser Photon. Rev.* **2**, 227–248 (2008).
5. Wang, J. et al. Reconfigurable radio-frequency arbitrary waveforms synthesized in a silicon photonic chip. *Nat. Commun.* **6**, 5957 (2015).
6. Nagatsuma, T., Ducournau, G. & Renaud, C. C. Advances in terahertz communications accelerated by photonics. *Nat. Photon.* **10**, 371–379 (2016).
7. Akyildiz, I. F., Jornet, J. M. & Han, C. Terahertz band: next frontier for wireless communications. *Phys. Comm.* **12**, 16–32 (2014).
8. Lamb, W. E. Theory of an optical maser. *Phys. Rev.* **134**, 1429–1450 (1964).
9. Agrawal, G. P. Population pulsations and nondegenerate four-wave mixing in semiconductor lasers and amplifiers. *J. Opt. Soc. Am. B* **5**, 147–159 (1988).
10. Hugi, A., Villares, G., Blaser, S., Liu, H. C. & Faist, J. Mid-infrared frequency comb based on a quantum cascade laser. *Nature* **492**, 229–233 (2012).
11. Villares, G., Hugi, A., Blaser, S. & Faist, J. Dual-comb spectroscopy based on quantum-cascade-laser frequency combs. *Nat. Commun.* **5**, 5192 (2014).
12. Burghoff, D. et al. Terahertz laser frequency combs. *Nat. Photon.* **8**, 462–467 (2014).
13. Lu, Q. Y. et al. High power frequency comb based on mid-infrared quantum cascade laser at $\lambda \sim 9$ μm. *Appl. Phys. Lett.* **106**, 051105 (2014).
14. Kippenberg, T. J., Holzwarth, R. & Diddams, S. A. Microresonator-based optical frequency combs. *Science* **332**, 555–559 (2011).
15. Wang, C. Y. et al. Mid-infrared optical frequency combs at 2.5 μm based on crystalline microresonators. *Nat. Commun.* **4**, 1345 (2013).
16. Del'Haye, P. et al. Phase-coherent microwave-to-optical link with a self-referenced microcomb. *Nat. Photon.* **10**, 516–520 (2016).
17. Faist, J. et al. Quantum cascade laser frequency combs. *Nanophotonics* **5**, 272–291 (2016).
18. Khurgin, J. B., Dikmelik, Y., Hugi, A. & Faist, J. Coherent frequency combs produced by self frequency modulation in quantum cascade lasers. *Appl. Phys. Lett.* **104**, 081118 (2014).
19. Mansuripur, T. S. et al. Single-mode instability in standing-wave lasers: the quantum cascade laser as a self-pumped parametric oscillator. *Phys. Rev. A* **94**, 063807 (2016).
20. Arahira, S., Matsui, Y. & Ogawa, Y. Mode-locking at very high repetition rates more than terahertz in passively mode-locked distributed-Bragg-reflector laser diodes. *IEEE J. Quant. Electron.* **32**, 1211–1224 (1996).
21. Villares, G. et al. Dispersion engineering of quantum cascade laser frequency combs. *Optica* **3**, 252 (2016).
22. Del'Haye, P., Schliesser, A. & Arcizet, O. Optical frequency comb generation from a monolithic microresonator. *Nature* **450**, 1214–1217 (2007).
23. Rösch, M. et al. On-chip, self-detected terahertz dual-comb source. *Appl. Phys. Lett.* **108**, 171104 (2016).
24. Hofstetter, D. & Faist, J. Measurement of semiconductor laser gain and dispersion curves utilizing Fourier transforms of the emission spectra. *IEEE Photon. Technol. Lett.* **11**, 1372–1374 (1999).
25. Petrov, V., Pyattaev, A., Moltchanov, D. & Koucheryavy, Y. Terahertz band communications: applications, research challenges, and standardization activities. *Proc. 8th International Congress on Ultra Modern Telecommunications and Control Systems and Workshops*, 183–190 (2016).
26. Hinkov, B., Hugi, A., Beck, M. & Faist, J. RF-modulation of mid-infrared distributed feedback quantum cascade lasers. *Opt. Express* **24**, 3294 (2016).

Acknowledgements

This work was supported by the DARPA SCOUT programme through grant no. W31P4Q-16-1-0002. The authors acknowledge support from the National Science Foundation under award no. ECCS-1614631. Any opinions, findings, conclusions or recommendations expressed in this material are those of the authors and do not necessarily reflect the views of the Assistant Secretary of Defense for Research and Engineering or of the National Science Foundation. M.P. and D.K. thank J.B. MacArthur for the assembly of RF filters, A.Y. Zhu for sputtering gold on a QCL submount, and N. Rubin for careful reading of the manuscript.

Author contributions

D.K. and M.P. conceived, designed and implemented the experiments and wrote the manuscript with feedback from the other co-authors. P.C. contributed to the realization of the experiments. F.X., C.Z. and K.L. provided the QCL devices. Y.W. and A.B. developed the theoretical model and contributed to the theoretical part of the manuscript. T.S.M., P.C., A.B., M.P., D.K. and F.C. discussed the data. All work was done under the supervision of F.C.

Competing interests

The authors declare no competing financial interests.

Additional information

Supplementary information is available for this paper at https://doi.org/10.1038/s41566-017-0026-y.

Reprints and permissions information is available at www.nature.com/reprints.

Correspondence and requests for materials should be addressed to M.P. or F.C.

Publisher's note: Springer Nature remains neutral with regard to jurisdictional claims in published maps and institutional affiliations.

Methods

QCLs. The devices used were continuous-wave, buried-heterostructure FP QCLs, fabricated using the same growth process and emitting at 4.5 µm (Thorlabs). They were coated with a high-reflectivity coating (reflectivity $R \approx 1$) on the back facet and an antireflection coating ($R \approx 0.01$) on the front facet. Due to the cavity asymmetry introduced by the coatings, the harmonic spectra produced by these lasers exhibit sidebands with much larger separation than that of nominally identical uncoated devices, a phenomenon attributed to a weaker population grating favouring coherent instability with larger sideband separation[19]. The single-stack active region consisted of strain-balanced $Ga_xIn_{1-x}As/Al_yIn_{1-y}As$ layers grown on an InP substrate[27]. The length and width of the buried waveguide were, respectively, 6 mm and 5 µm. The spectral evolution of device QCL_1 is reported in ref. [19](TL-4.6:HR/AR), while that of QCL_2 is provided in Supplementary Section I. The QCLs were driven with low-noise current drivers (Wavelength Electronics QCL LAB 2000) with an average specified current noise density of 4 nA $Hz^{-1/2}$ and with their temperature stabilized using low-thermal-drift temperature controllers (Wavelength Electronics TC5) with typical fluctuations smaller than 10 mK.

Multiheterodyne set-up. Two different configurations were used for the multiheterodyne experiment: self-detection and external detection modes. In the first scheme (Fig. 3f), the beam emitted from a QCL operating in the harmonic regime ($I_{QCL1} = 1{,}008$ mA, where I is the electrical current injected in the laser) was collimated using an off-axis parabolic mirror (25.4 mm focal length) and sent through a Faraday isolator (Innovation Photonics, 30 dB extinction ratio) to prevent feedback-induced destabilization of the harmonic state. A beam reducer was used to decrease the beam diameter and maximize its transmission through the isolator. After partial attenuation by a neutral density filter the beam was focused inside the cavity of a second QCL acting simultaneously as a reference comb and a fast photomixer ($I_{QCL2} = 1{,}015$ mA). By using a beamsplitter (45:55 splitting ratio) and a flip mirror, one can selectively measure with a Fourier transform infrared (FTIR) spectrometer (Bruker Vertex 80v, 0.1 cm^{-1} resolution) the optical spectra of the harmonic comb, and the reference comb, upon injection. In the external detection mode (Supplementary Fig. 3a), both QCLs were free-running, one operating in the harmonic regime ($I_{QCL1} = 1{,}139$ mA) and the other as a reference comb ($I_{QCL2} = 1{,}084$ mA), and the two collinear beams were focused onto an external fast HgCdTe (MCT) detector (Vigo PVI-2TE-5, 1 GHz bandwidth). The detector was tilted at an angle to minimize optical feedback on the lasers. In both configurations, the beating of the optical fields, whether occurring inside the cavity of the QCL detector or on the fast photodetector, was converted into an RF signal, which was sent to the RF circuit shown in Fig. 3f. An RF bias-tee was used to extract the multiheterodyne signal from the QCL detector. The RF signal was amplified and then downconverted using an RF mixer. The local oscillator (LO) signal was supplied by a tunable signal generator (R&S SMF100A). While monitoring the RF signal on the spectrum analyser it was possible to tune the central frequency of the multiheterodyne spectrum by adjusting the LO frequency and the spacing between individual tones by tuning the currents of the two QCLs. This allowed three adjacent beatnotes of the spectrum to be aligned within the passbands (60 MHz) of three homemade filters, centred at 50 MHz, 135 MHz and 220 MHz. The filtered signals were amplified and their frequency measured using three synchronized frequency counters (Agilent 53220A) sharing the same external gate and trigger control and a 10 MHz clock reference. To verify the synchronization of the frequency counters we adopted the following method. A frequency-modulated (FM) waveform (15 MHz carrier frequency, 1 Hz modulation, 1 kHz maximum frequency deviation) was sent to the three counters. The gate time of the counters was chosen to be the same as in the multiheterodyne experiment, and the frequency of the FM waveform was measured over a total acquisition time of 200 s. The traces acquired by the counters were analysed and the resulting statistics describing the deviation from equal readings of the counters gave a standard deviation smaller than 100 mHz and a mean value of 0 Hz.

Active stabilization of the multiheterodyne signal, as demonstrated in ref. [11],could improve, by orders of magnitude, the frequency stability of the multiheterodyne beat spectrum by compensating the slow frequency drifts of the signal. However, its implementation in the present work was not necessary as the achieved relative accuracy without active stabilization can be considered to be largely sufficient to prove the occurrence of locking among the modes of the harmonic state.

Data availability. The data that support the plots within this paper and other findings of this study are available from the corresponding author upon reasonable request.

References

27. Xie, F. et al. Room temperature CW operation of short wavelength quantum cascade lasers made of strain balanced $Ga_xIn_{1-x}As/Al_yIn_{1-y}As$ material on InP substrates. *IEEE J. Sel. Topics Quantum Electron.* **17**, 1445–1452 (2011).